Journal of the Korean Ceramic Society
Vol. 40, No. 6, pp. 507~512, 2003.

Synthesis of Cathode Materials $LiNi_{1-y}Co_yO_2$ from Various Starting Materials and their Electrochemical Properties

Myoung Youp Song,† Ho Rim, Eui Yong Bang, Seong Gu Kang,* and Soon Ho Chang*

Division of Advanced Materials Engineering, Research Center of Industrial Technology, Engineering Research Institute, Chonbuk National University, Chonju 561-756, Korea
**Electronics and Telecommunications Research Institute, Taejon 305-350, Korea*
(Received March 27, 2003; Accepted May 13, 2003)

ABSTRACT

The $LiNi_{1-y}Co_yO_2$ samples were synthesized at 800°C and 850°C, by the solid-state reaction method, from the various starting materials LiOH, Li_2CO_3, NiO, $NiCO_3$, Co_3O_4, $CoCO_3$, and their electrochemical properties are investigated. The $LiNi_{1-y}Co_yO_2$ prepared from Li_2CO_3, NiO, and Co_3O_4 exhibited the α-$NaFeO_2$ structure of the rhombohedral system (space group; $R\bar{3}m$). As the Co content increased, the lattice parameters a and c decreased. The reason is that the radius of Co ion is smaller than that of Ni ion. The increase in c/a shows that two-dimensional structure develops better as the Co content increases. The $LiNi_{0.7}Co_{0.3}O_2$ [HOO(800,0.3)] synthesized at 800°C from LiOH, NiO, and Co_3O_4 exhibited the largest first discharge capacity 162 mAh/g. The size of particles increases roughly as the valve of y increases. The samples with the larger particles have the larger first discharge capacities. The cycling performances of the samples with the first discharge capacity larger than 150 mAh/g were investigated. The $LiNi_{0.9}Co_{0.1}O_2$[COO(850,0.1)] synthesized at 850°C from Li_2CO_3, NiO, and Co_3O_4 showed an excellent cycling performance. The sample with the larger first discharge capacity will be under the more severe lattice destruction, due to the expansion and contraction of the lattice during intercalation and deintercalation, than the sample with the smaller first discharge capacity. As the first discharge capacity increases, the capacity fading rate thus increases.

Key words : $LiNi_{1-y}Co_yO_2$, Solid-state reaction method, Various starting materials, The 1st discharge capacity, Cycling performance, Lattice destruction

1. Introduction

Transition metal oxides such as $LiMn_2O_4$,[1-4] $LiCoO_2$, and $LiNiO_2$ have been investigated in order to apply them as positive electrode (cathode) materials for lithium secondary batteries. $LiMn_2O_4$ is very cheap and does not bring about environmental pollution, but its cycle performance is not good. $LiNiO_2$ and $LiCoO_2$ exhibit complementary behaviour; $LiCoO_2$ is easy to prepare but is very expensive while $LiNiO_2$ is cheaper but is quite difficult to prepare in a very reproductive way as a result of a tendency to nonstoichiometry due to the presence of an excess of nickel.[5,6]

A convenient way to overcome these drawbacks may be to use mixed phases with $LiNi_{1-y}Co_yO_2$ composition because the presence of cobalt stabilizes the structure in a strictly two-dimensional fashion, thus favouring good reversibility of the intercalation and deintercalation reactions.[7-16]

In this work, $LiNi_{1-y}Co_yO_2$ (y=0.1, 0.3, 0.5, 0.7, and 1.0) were synthesized by the solid-state reaction method at different temperatures from various starting materials. The crystal structure, the electrochemical properties and the microstructure of the synthesized samples were examined. The synthesis conditions (the kind of starting materials, composition and temperature) for the excellent electrochemical properties were investigated.

†Corresponding author : Myoung Youp Song
E-mail : songmy@moak.chonbuk.ac.kr
Tel : +82-63-270-2379 Fax : +82-63-270-2386

2. Experimental

LiOH, Li_2CO_3, NiO, $NiCO_3$, Co_3O_4, and $CoCO_3$ were used as starting materials in order to synthesize $LiNi_{1-y}Co_yO_2$ by the solid-state reaction method. All the starting materials (with the purity 99.9%) were purchased from Aldrich Co.

The experimental procedure of this work is given schematically in Fig. 1. The mixture of starting materials in the compositions $LiNi_{1-y}Co_yO_2$ (y=0.1, 0.3, 0.5, 0.7, and 1.0) was mixed sufficiently and pelletized. This pellet was heat-treated in air at 650°C for 20 h. It was then ground, mixed, pelletized and calcined at 800°C or 850°C for 20 h. This pellet was cooled at a cooling rate 50°C/min, ground, mixed and again pelletized. It was then calcined again at 800°C or 850°C for 20 h.

Table 1 gives starting materials, calcining temperature and the value of y in $LiNi_{1-y}Co_yO_2$ for the prepared samples. The designated names for these samples are also indicated.

The phase identification of the synthesized samples was carried out by X-Ray Diffraction (XRD) analysis using Cu K_α radiation (Mac-Science Co., Ltd.). The scanning rate was

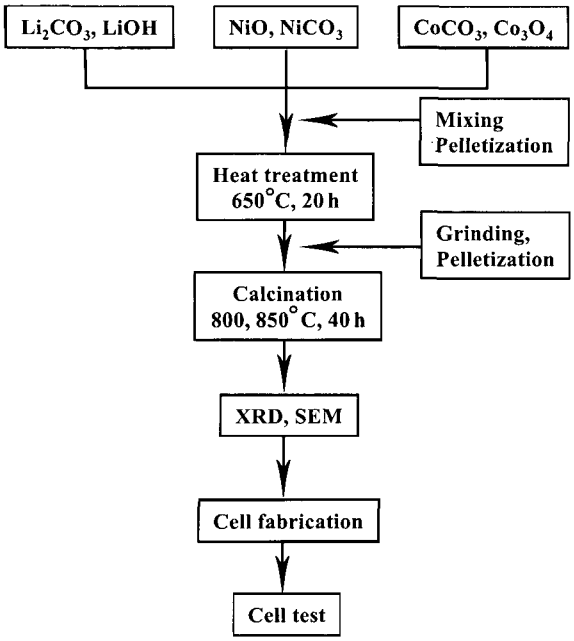

Fig. 1. Experimental procedure.

Table 1. Starting Materials, Calcining Temperature, the Value of y in $LiNi_{1-y}Co_yO_2$ for the Prepared Samples, and their Designated Names

Starting materials	Calcining temp. (°C)	y	Name*
LiOH, NiO, Co_3O_4	800	0.1	HOO(800,0.1)
		0.3	HOO(800,0.3)
		0.5	HOO(800,0.5)
LiOH, NiO, Co_3O_4	850	0.1	HOO(850,0.1)
		0.3	HOO(850,0.3)
		0.5	HOO(850,0.5)
Li_2CO_3, NiO, Co_3O_4	800	0.1	COO(800,0.1)
		0.3	COO(800,0.3)
		0.5	COO(800,0.5)
Li_2CO_3, NiO, Co_3O_4	850	0.1	COO(850,0.1)
		0.3	COO(850,0.3)
		0.5	COO(850,0.5)
Li_2CO_3, NiO, $CoCO_3$	800	0.1	COC (800,0.1)
		0.3	COC (800,0.3)
		0.5	COC (800,0.5)
Li_2CO_3, NiO, $CoCO_3$	850	0.1	COC (850,0.1)
		0.3	COC (850,0.3)
		0.5	COC (850,0.5)
Li_2CO_3, $NiCO_3$, Co_3O_4	800	0.1	CCO (800,0.1)
		0.3	CCO (800,0.3)
		0.5	CCO (800,0.5)
Li_2CO_3, $NiCO_3$, Co_3O_4	850	0.1	CCO (850,0.1)
		0.3	CCO (850,0.3)
		0.5	CCO (850,0.5)
Li_2CO_3, $NiCO_3$, $CoCO_3$	800	0.1	CCC (800,0.1)
		0.3	CCC (800,0.3)
		0.5	CCC (800,0.5)
Li_2CO_3, $NiCO_3$, $CoCO_3$	850	0.1	CCC (850,0.1)
		0.3	CCC (850,0.3)
		0.5	CCC (850,0.5)

*H indicates the hydroxide, O the oxide and C the carbonate.

16°/min and the scanning range of diffraction angle (2θ) is 10°≤2θ≤70°. The morphologies of the samples were observed using a Scanning Electron Microscope (SEM).

The electrochemical cells consisted of $LiNi_{1-y}Co_yO_2$ as a positive electrode, Li foil as a negative electrode, and electrolyte of 1 M $LiPF_6$ in a 1 : 1 (volume ratio) mixture of Ethylene Carbonate (EC) and Dimethyl Carbonate (DMC). A Whatman glass-fiber was used as the separator. The cells were assembled in an argon-filled dry box. To fabricate the positive electrode, 89 wt% synthesized oxide, 10 wt% acetylene black, and 1 wt% Polytetrafluoroethylene (PTFE) binder were mixed in an agate mortar. By introducing Li metal, Whatman glass-fiber, positive electrode, and the electrolyte, the cell was assembled. All the electrochemical tests were performed at room temperature with a potentiostatic/galvanostatic system (Mac-Pile system, Bio-Logic Co. Ltd.). The cells were cycled at a current density of 200 μA/cm^2 between 3.2 and 4.3 V.

3. Results and Discussion

Fig. 2 shows the X-ray diffraction patterns of the $LiNi_{1-y}Co_yO_2$[COO(800)] synthesized at 800°C from Li_2CO_3, NiO, and Co_3O_4. They were identified as the α-$NaFeO_2$ structure of the rhombohedral system (space group; $R\bar{3}m$). As the Co content increases, the relative intensity of (003) to (104) increases. The reason is that the directionality to the c-axis gets better since the $LiCoO_2$ layer increases in which Li and Co ions are in a completely-ordered arrangement, and since the three-dimensional characteristics decreases which results from the substitution of Ni ions for Li sites like $LiNiO_2$.

Fig. 3 shows the parameters of the hexagonal unit cell, a and c, and the degree of trigonal distortion, c/a, versus Co content y in the $LiNi_{1-y}Co_yO_2$[COO(800)]. As the Co content increases, the lattice parameters a and c decrease. The reason is that the radius of Co ion[0.53 Å(low spin)] is smaller

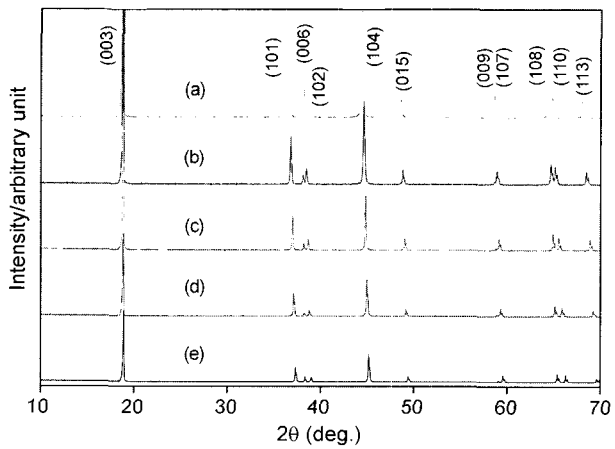

Fig. 2. X-ray(CuKα) diffraction patterns of (a) $LiNi_{0.9}Co_{0.1}O_2$, (b) $LiNi_{0.7}Co_{0.3}O_2$, (c) $LiNi_{0.5}Co_{0.5}O_2$, (d) $LiNi_{0.3}Co_{0.7}O_2$, and (e) $LiCoO_2$[COO(800)] synthesized at 800°C from Li_2CO_3, NiO, and Co_3O_4.

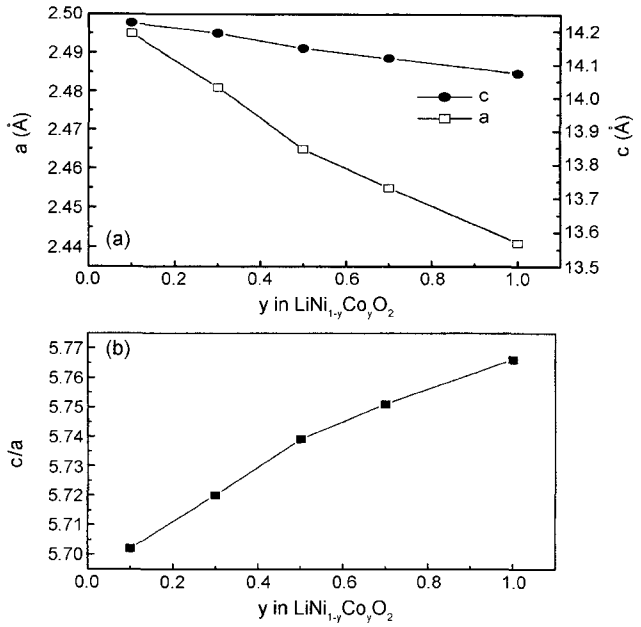

Fig. 3. Parameters of the hexagonal unit cell, a, c and degree of trigonal distortion, c/a, versus Co content y in $LiNi_{1-y}Co_yO_2$; (a) hexagonal lattice parameters, a(□) and c(●), and (b) (c/a) ratio versus Co content y in $LiNi_{1-y}Co_yO_2$ [COO(800)].

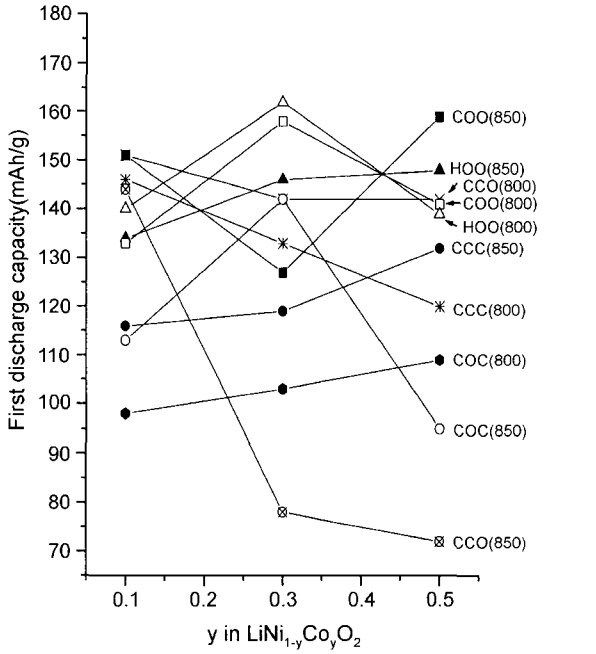

Fig. 4. Variations of the first discharge capacities of the synthesized samples with compositions, starting materials and synthetic temperatures.

than that of Ni ion[0.60 Å(low spin)]. However, the c-axis is less contracted compared with a-axis, showing that the two-dimensional structure develops better than $LiNiO_2$.

Fig. 4 shows the variations of the first discharge capacities of the synthesized samples with composition, starting materials and synthetic temperature. The $LiNi_{0.7}Co_{0.3}O_2$[HOO (800,0.3)] synthesized at 800°C from LiOH, NiO, and Co_3O_4

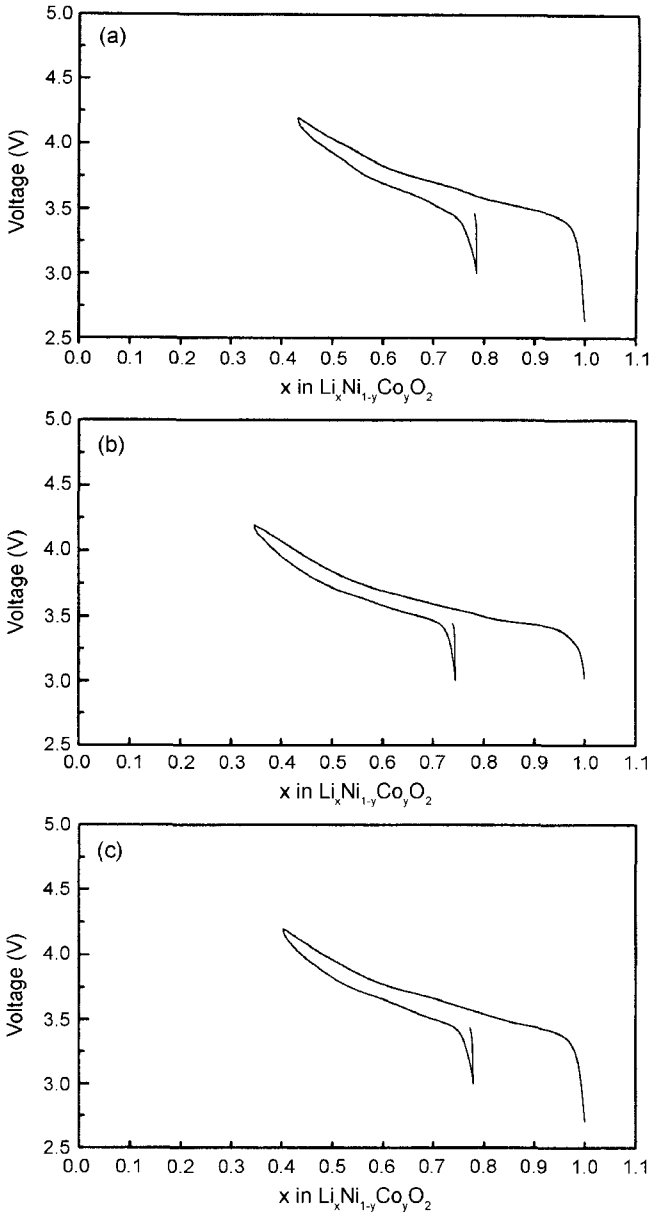

Fig. 5. Curves for voltage vs.x in $Li_xNi_{1-y}Co_yO_2$ of $Li/LiNi_{1-y}Co_yO_2$ [COC(800)] cells prepared at 800°C from Li_2CO_3, NiO, and $CoCO_3$; (a) y=0.1, (b) y=0.3, and (c) y=0.5.

had the largest first discharge capacity 162 mAh/g. The $LiNi_{0.7}Co_{0.3}O_2$[COO(800,0.3)] synthesized at 800°C from Li_2CO_3, NiO, and Co_3O_4, the $LiNi_{0.5}Co_{0.5}O_2$[COO(850,0.5)] and the $LiNi_{0.9}Co_{0.1}O_2$[COO(850,0.1)] synthesized at 850°C from Li_2CO_3, NiO, and Co_3O_4, and the $LiNi_{0.9}Co_{0.1}O_2$[CCO (800,0.1)] synthesized at 800°C from Li_2CO_3, $NiCO_3$, and Co_3O_4, also had the first discharge capacities larger than 150 mAh/g.

Fig. 5 shows the curves for voltage vs. x in $Li_xNi_{1-y}Co_yO_2$ of $Li/LiNi_{1-y}Co_yO_2$[COC(800)] cells prepared at 800°C from Li_2CO_3, NiO, and $CoCO_3$ for (a) y=0.1, (b) y=0.3, and (c) y=0.5. These samples exhibited relatively small first discharge capacities (smaller than 109 mAh/g). The Δx in

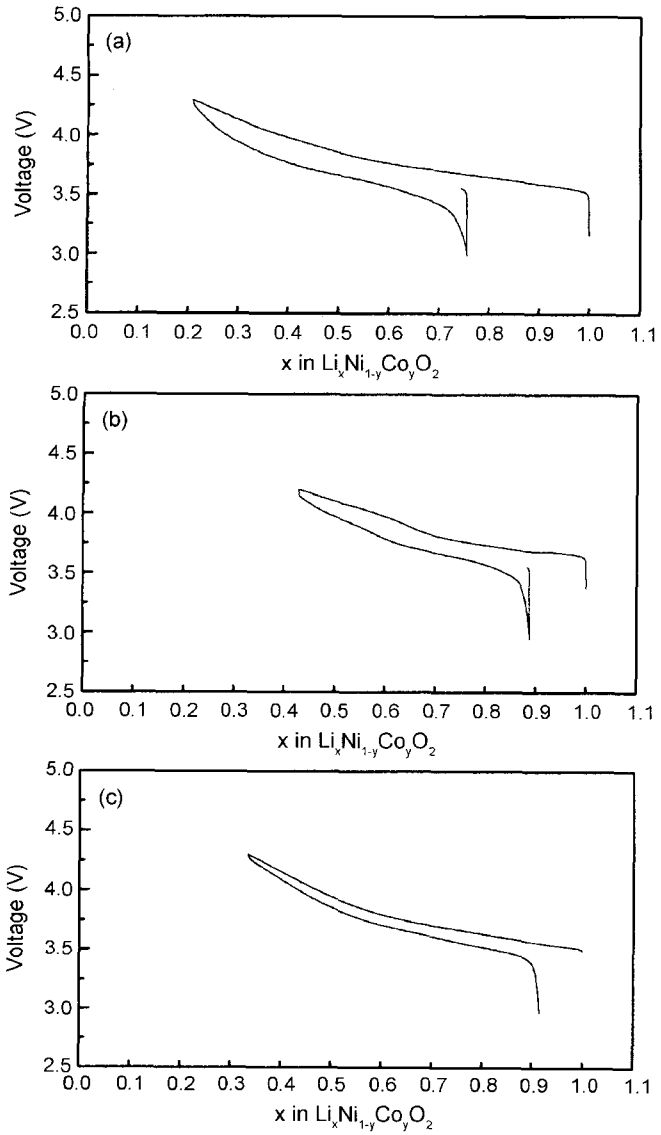

Fig. 6. Curves for voltage vs.x in $Li_xNi_{1-y}Co_yO_2$ of $Li/LiNi_{1-y}Co_yO_2$ [COO(850)] cells prepared at 850°C from Li_2CO_3, NiO, and Co_3O_4; (a) y=0.1, (b) y=0.3, and (c) y=0.5.

$Li_xNi_{1-y}Co_yO_2$ for the discharge curve is naturally proportional to the first discharge capacity. The plateau in the voltage vs. x curve is not distinct. As compared with the quantity of the deintercalated Li ions by the first charging, that of the intercalated Li ions by the first discharging is much smaller. It is considered that, during the first charging, deintercalation of Li ions from unstable 3b sites destructs the $LiNiO_2$ structure (α-$NaFeO_2$ structure), leading to a smaller quantity of the following intercalation.

Fig. 6 shows the curves for voltage vs. x in $Li_xNi_{1-y}Co_yO_2$ of $Li/LiNi_{1-y}Co_yO_2$[COO(850)] cells prepared at 850°C from Li_2CO_3, NiO, and Co_3O_4 for (a) y=0.1, (b) y=0.3, and (c) y=0.5. These samples exhibited relatively large first discharge capacities (larger than 127 mAh/g). The plateau in the voltage vs. x curve is more distinct as compared with the curves in Fig. 5.

Fig. 7 shows the SEM micrographs of $LiNi_{1-y}Co_yO_2$[COC (800)] prepared at 800°C from Li_2CO_3, NiO, and $CoCO_3$ for (a) y=0.1, (b) y=0.3, and (c) y=0.5. These are for the same samples in Fig. 5. As the content of Co increases from y=0.1 to y=0.3, the size of particles becomes smaller. The particles then grows when y increases from y=0.3 to 0.5. The particles for y=0.5 have the largest size among three samples.

Fig. 8 shows SEM micrographs of $LiNi_{1-y}Co_yO_2$[COO(850)] prepared at 850°C from Li_2CO_3, NiO, and Co_3O_4 for (a) y=0.1, (b) y=0.3, and (c) y=0.5. These are for the samples in Fig. 6. When the value of y increases from y=0.1 to 0.3, the size of particles becomes a little smaller. The particles then grow into the largest ones when y increase from y=0.3 to 0.5.

A comparision of Fig. 8 with Fig. 6 shows that the size of Δx, which is naturally proportional to the first discharge capacity, increases as the size of particles increases.

Figs. 6 and 8 show that the size of particles increases roughly as the value of y increases.

The samples in Fig. 8 have larger first discharge capacities than those in Fig. 7. This agrees well to the point that the samples with the larger particles have the larger first discharge capacities.

For these samples, the variations of the discharge capaci-

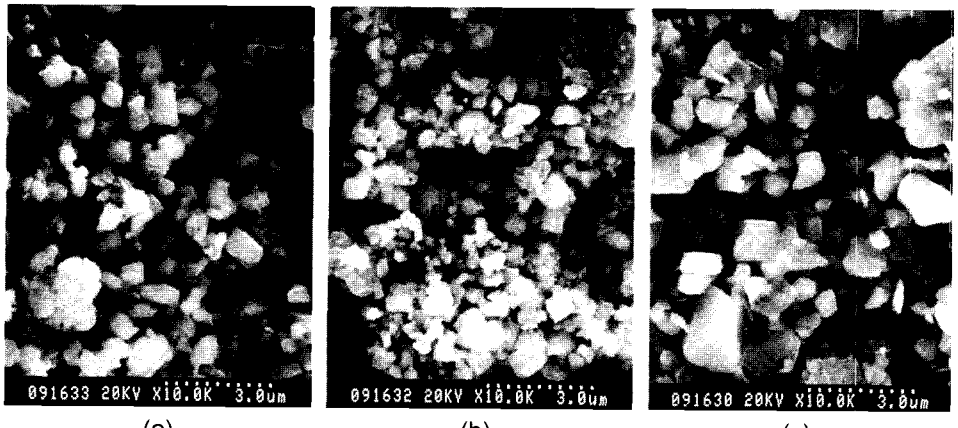

Fig. 7. SEM micrographs of $LiNi_{1-y}Co_yO_2$[COC(800)] prepared at 800°C from Li_2CO_3, NiO, and $CoCO_3$; (a) y=0.1, (b) y=0.3, and (c) y=0.5.

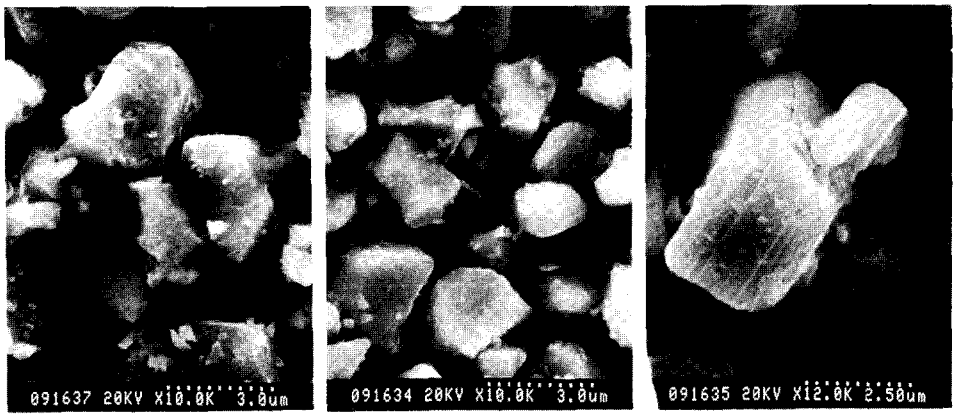

Fig. 8. SEM micrographs of $LiNi_{1-y}Co_yO_2$[COO(850)] prepared at 850°C from Li_2CO_3, NiO, and Co_3O_4; (a) y=0.1, (b) y=0.3, and (c) y=0.5.

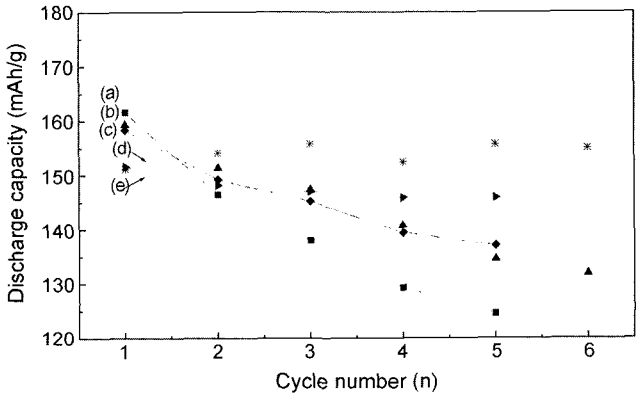

Fig. 9. Variations of the discharge capacities with the number of discharge cycle; (a) $LiNi_{0.7}Co_{0.3}O_2$[HOO(800)] synthesized at 800°C from LiOH, NiO, and Co_3O_4, (b) $LiNi_{0.5}Co_{0.5}O_2$[COO(850,0.5)] synthesized at 850°C, (c) $LiNi_{0.7}Co_{0.3}O_2$[COO(800,0.3)] synthesized at 800°C, (d) $LiNi_{0.9}Co_{0.1}O_2$[COO(850,0.1)] synthesized at 850°C from Li_2CO_3, NiO, and Co_3O_4, and (e) $LiNi_{0.9}Co_{0.1}O_2$ [CCO(800,0.1)] synthesized at 800°C from $LiCO_3$, $NiCO_3$, and Co_3O_4.

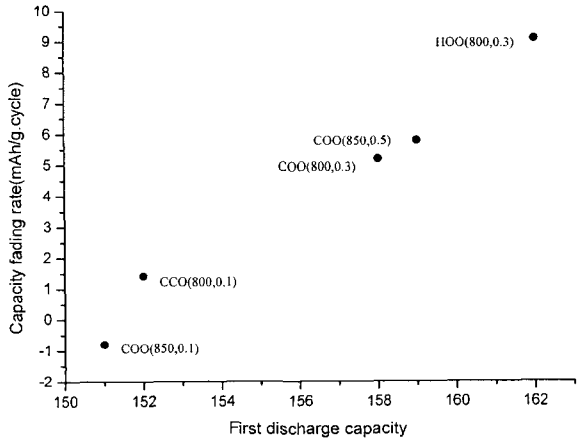

Fig. 10. Variation of capacity fading rate with the first discharge capacity for the samples with the first discharge capacity larger than 150 mAh/g. The starting materials and the synthetic temperature are also indicated.

ties with the number of discharge cycle are given in Fig. 9. The $LiNi_{0.9}Co_{0.1}O_2$[COO(850,0.1)] synthesized at 850°C from Li_2CO_3, NiO, and Co_3O_4 exhibited an excellent cycling performance with the discharge capacity about 156 mAh/g at the 6th discharge cycle. The $LiNi_{0.9}Co_{0.1}O_2$[CCO(800,0.1)] synthesized at 800°C from Li_2CO_3, $NiCO_3$, and Co_3O_4 also had an excellent cycling performance.

Fig. 10 shows the variations of capacity fading rate with the first discharge capacity for the samples with the first discharge capacity larger than 150 mAh/g. The starting materials and the synthetic temperature are also indicated. As the first discharge capacity increases, the capacity fading rate increases. The expansion and contraction of the $LiNi_{1-y}Co_yO_2$ due to the intercalation and deintercalation make the unit cell strained and distorted. With cycling, the interstitial sites and thus the $LiNi_{1-y}Co_yO_2$ structure will be destroyed. This leads to the capacity fading of $LiNi_{1-y}Co_yO_2$ with cycling. The sample with the larger first discharge capacity will be under the more severe lattice destruction than the sample with the smaller first discharge capacity, causing the larger capacity fading rate of the samples.

4. Conclusions

The $LiNi_{1-y}Co_yO_2$ samples were synthesized at 800°C and 850°C, by the solid-state reaction method, from the various starting materials LiOH, Li_2CO_3, NiO, $NiCO_3$, Co_3O_4, and $CoCO_3$. The $LiNi_{1-y}Co_yO_2$ prepared from Li_2CO_3, NiO, and Co_3O_4 exhibited the α-$NaFeO_2$ structure of the rhombohedral system (space group; $R\bar{3}m$). As the Co content increased, the lattice parameters a and c decreased. The reason is that the radius of Co ion is smaller than that of Ni ion. The increase in c/a shows that two-dimensional structure develops better as the Co content increases. The $LiNi_{0.7}Co_{0.3}O_2$[HOO(800,0.3)] synthesized at 800°C from LiOH, NiO, and Co_3O_4 exhibited the largest first discharge capacity 162 mAh/g. The size of particles increases roughly as the valve of y increases. The samples with the larger particles have the larger first discharge capacities. The $LiNi_{0.9}Co_{0.1}O_2$[COO(850,0.1)] synthe-

sized at 850°C from Li_2CO_3, NiO, and Co_3O_4 showed an excellent cycling performance. The sample with the larger first discharge capacity will be under the more severe lattice destruction, due to the expansion and contraction of the lattice during intercalation and deintercalation, than the sample with the smaller first discharge capacity. As the first discharge capacity increases, the capacity fading rate thus increases.

Acknowledgement

This work was supported by the Research Center of Industrial Technology, Engineering Research Institute at Chonbuk National University.

REFERENCES

1. Y. K. Choi and B. H. Kim, "Synthesis of $LiMn_2O_4$ Cathod Materials by Emulsion Drying Method and its Electrochemical Properties," *J. Kor. Ceram.*, **5** 250-54 (1999).
2. B. W. Lee and S. H. Kim, "Wetchemical Preparation of Li-rich $LiMn_2O_4$ Spinel by Oxalate Precipitation," *J. Kor. Ceram. Soc.*, **36** 698-704 (1999).
3. Y. S. Han, J. T. Son, H. G. Kim, and H. T. Jung, "Combustion Synthesis of $LiMn_2O_4$ with Citric Acid and the Effect of Post-heat Treatment," *J. Kor. Ceram. Soc.*, **38** 301-07 (2001).
4. M. Y. Song and M. S. Shon, "Variations of the Electrochemical Properties of $LiMn_2O_4$ with the Calcining Temperature," *J. Kor. Ceram. Soc.*, **39** [6] 523-27 (2002).
5. J. R. Dahn, U. von Sacken, M. R. Jukow, and H. Aljanaby, "Rechargeable $LiNiO_2$/Carbon Cells," *J. Electrochem. Soc.*, **138** 2207-12 (1991).
6. M. Y. Song and R. Lee, "Synthesis by Sol-gel Method and Electrochemical Properties of $LiNiO_2$ Cathode Material for Lithium Secondary Battery," *J. Power Sources*, **4863** 1-7 (2002).
7. S. J. Lee, J. K. Lee, D. W. Kim, and H. K. Baik, "Fabrication of Thin Film $LiCo_{0.5}Ni_{0.5}O_2$ Cathode for Li Rechargeable Microbattery," *J. Electrochem. Soc.*, **143** [11] L268-70 (1996).
8. R. Alcantara, J. Morales, and J. L. Tirado, "Electrochemical Science and Technology Structure and Electrochemical Properties of $Li_{1-x}(Ni_yCo_{1-y})_{1+x}O_2$ Effect of Chemical Delithiation at 0°C," *J. Electrochem. Soc.*, **142** [12] 3997-4005 (1995).
9. A. Ueda and T. Ohzuku, "Solid-state Redox Reactions of $LiNi_{1/2}Co_{1/2}O_2(R\bar{3}m)$ for 4 Volt Secondary Lithium Cells," *J. Electrochem. Soc.*, **141** [8] 2010-14 (1994).
10. A. Rougier, I. Saadoune, P. Gravereau, P. Willmann, and C. Delmas, "Effect of Cobalt Substitution on Cation Distribution in $LiNi_{1-y}Co_yO_2$ Electrode Materials," *Solid State Ionics*, **90** 83-90 (1996).
11. Y. M. Choi, S. I. Pyun, and S. I. Moon, "Effect of Cation Mixing on the Electrochemical Lithium Intercalation Reaction into Porous $Li_{1-x}Ni_{1-y}Co_yO_2$ Elcetrodes," *Solid State Ionics*, **89** 43-52 (1996).
12. E. Zhecheva and R. Stoyanova, "Stabilization of the Layered Crystal Structure of $LiNiO_2$ by Co-substitution," *Solid State Ionics*, **66** 143-49 (1993).
13. C. Delmas and I. Saadoune, "Electrochemical and Physical Properties of the $Li_xNi_{1-y}Co_yO_2$ Phases," *Solid State Ionics*, **53-56** 370-75 (1992).
14. M. Menetrier, A. Rougier, and C. Delmas, "Cobalt Segregation in the $LiNi_{1-y}Co_yO_2$ Solid Solution : A Preliminart Li NMR Study," *Solid State Comm.*, **90** [7] 439-42 (1994).
15. B. Banov, J. Bourilkov, and M. Mladenov, "Cobalt Stabilized Layered Lithium-nickel Oxides, Cathodes in Lithium Rechargeable Cells," *J. Power Sources*, **54** 268-70 (1995).
16. C. Delmas, I. Saadoune, and A. Rougier, "The Cycling Properties of the $Li_xNi_{1-y}Co_yO_2$ Electrode," *J. Power Sources*, **43-44** 595-602 (1993).